

Supporting Information

Energy harvesting textiles: using wearable luminescent solar concentrators to improve the efficiency of fiber solar cells

Chieh-Szu Huang, Xinyue Kang, René M. Rossi, Maksym V. Kovalenko, Xuemei Sun, Huisheng Peng, and Luciano F. Boesel**

1. Experimental and synthesis details
 - 1.1 Fiber solar cells fabrication
 - 1.2 Amphiphilic polymer connetworks synthesis
2. Solar cells power conversion efficiency
 - 2.1 Raw data
 - 2.2 Statistics
 - 2.3 EQE and dark current
 - 2.4 Double-sided LSCs PCE enhancement
 - 2.5 Experimental and simulated photon numbers comparison
 - 2.6 Parameters and defining equations
3. Simulation
 - 3.1 Monte-Carlo ray-tracing
 - 3.2 Ray-tracing screening for optimal photon harvesting
 - 3.3 Ray-tracing screening for various LSCs width photon harvesting

1. Experimental details

1.1 Fabrication of fiber solar cells

1.1.1 Preparation of photoanode fiber

A Ti wire (diameter of 127 μm , Alfa Aesar) was sequentially cleaned by sonication in acetone, isopropanol and deionized water for 10 min each. Then TiO_2 nanotube arrays were grown on Ti wire by an anodic oxidation in a water bath. A 0.3 wt% NH_4F /ethylene glycol (Sinopharm) solution containing 8 wt% H_2O was prepared as the electrolyte. The growth was operated in a two-electrode system with Ti wire as anode and Pt plate as cathode at 60 V for 6 h. Then, the modified Ti wire was washed with deionized water and annealed at 500 $^\circ\text{C}$ for 60 min in the furnace. After cooled to room temperature, the wire was treated with 100 mM TiCl_4 (Macklin) aqueous solution at 70 $^\circ\text{C}$ for 30 min and rinsed using deionized water. The as-prepared wire was annealed at 450 $^\circ\text{C}$ for 30 min. After cooled to 110 $^\circ\text{C}$, the wire was immersed in N719 or Y123 (Yingkou OPV Tech New Energy Co., Ltd.) solution (0.3 mM or 0.1 mM, mixture solvent of dehydrated acetonitrile (Adamas) and tert-butanol (Sinopharm) with an equal volume ratio) for 16 h at least.

1.1.2 Preparation of counter electrode fiber

Carbon nanotube (CNT) ribbon was synthesized by floating catalyst chemical vapor deposition method. In a reducing hydrogen atmosphere, the CNTs formed aerogel in the hot zone of a furnace (1200 $^\circ\text{C}$) and the aerogel was collected into cylindrical hollow socks. The CNT sock was pulled out of the furnace and then densified through water. The CNT sock shrank immediately into CNT ribbon upon arriving at the water surface. Then it was dried, twisted and collected onto a spool to produce the CNT fiber (typical diameter of 50 μm).

1.1.3 Fabrication of fiber DSSC

The as-prepared dye-absorbed Ti/TiO₂ wire was twisted with CNT fiber and then was set into a flexible, transparent and polyethylene capillary tube with an inner diameter of 600 μm and an outer diameter of 1000 μm. After injecting the redox electrolyte with a syringe, the tube was sealed by heating. All SEM images were taken by field emission scanning electron microscope (Ultra 55, Zeiss) operated at 5 kV.

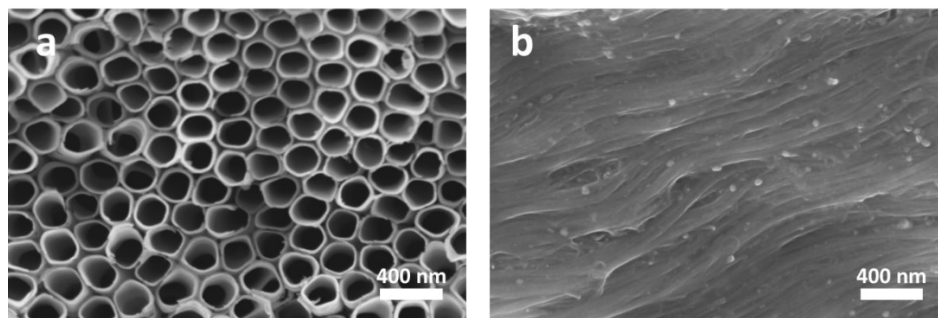


Figure S1. SEM images of (a) TiO₂ nanotube arrays and (b) CNT fiber surface morphology.

1.2 Amphiphilic polymer conetworks synthesis scheme

1.2.1 Materials details

Methacryloxypropyl-terminated poly(dimethylsiloxane) (MA-PDMS-MA, viscosity 50–90 cSt, 4500–5500 g mol⁻¹, ¹H NMR: M_n = 4600 g mol⁻¹, GPC: M_n = 3500 g mol⁻¹, PDI = 1.7 with GPC and NMR characterization reported previously^[1]) was purchased from ABCR, Germany. Trimethylsilyl hydroxyethyl acrylate (TMS-HEA) were prepared according to previously reported procedures ^[1] and stored under argon at -20 °C until use. The UV-initiator (2,2-Dimethoxy-2-phenyl acetophenone) and Cormarin 6 were purchased from Sigma-Aldrich, Switzerland. All the solvents were provided by Sigma-Aldrich, Switzerland or Biosolve Chimie, The Netherlands and used as received. The water was Milli-Q water from an in-house supply.

1.2.2 Synthesis route

The synthesis of preAPCNs via crosslinking TMS capped HEA and MA-PDMS-MA was based on a protocol previously developed in our group. The stoichiometry of the UV-initiator in this work is 3 mol. %, according to the data sheet provided by the supplier. The deprotection of the TMS groups was performed by immersing preAPCNs overnight in a 1:1 mixture of water and isopropanol which was acidified with concentrated HCl. The preAPCNs and APCNs films are washed in THF, acetone, and ethanol, respectively for 3 hr between each step to remove extra residuals. The hydrophobic dye, Coumarin 6 (C6), is loaded under 0.2 w/v % via 3 hours swelling of the APCNs films in toluene solution.

Coumarins are well-known in LSCs research due to their high quantum yield, large Stoke shift, and good photostability. The absorbance maximum of C6 is at 455 nm and the emission maximum is at 520 nm, hence the Stoke shift of the loaded C6 in LSCs is 65 nm. The absolute values of PL QY were measured 86% by using a Quantaurus-QY spectrometer from Hamamatsu in powder mode.

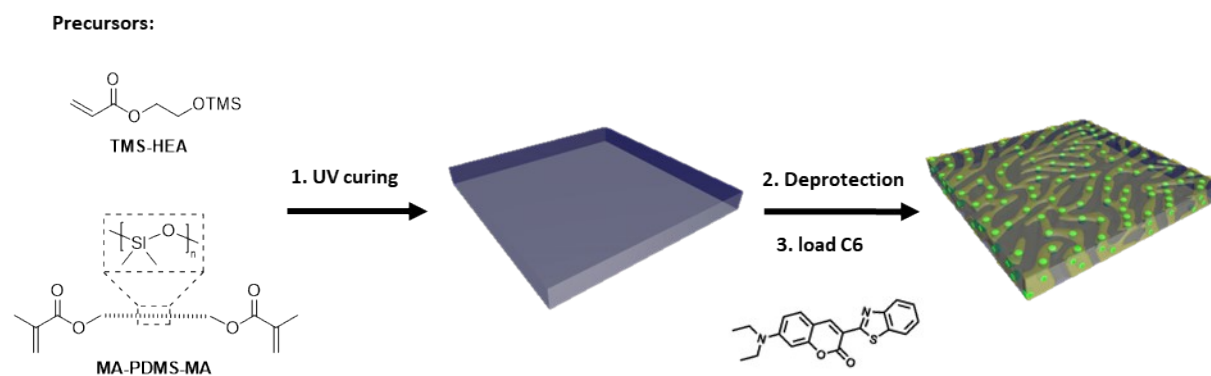


Figure S2. Synthesis scheme of APCNs containing C6.

1.2.3 Water vapor permeation

The water vapor permeation ability of APCNs is carried out with the comparison with flexible polymer PDMS at 35 and 80 °C. Samples are measured via covering a glass vial with 0.5 cm diameter opening filled with 3 g water, put into the oven, and measuring the lost weight after

respect time. All samples are sealed with wax at the joint of polymer film and vial opening, to avoid water vapor escaped from non-film areas.

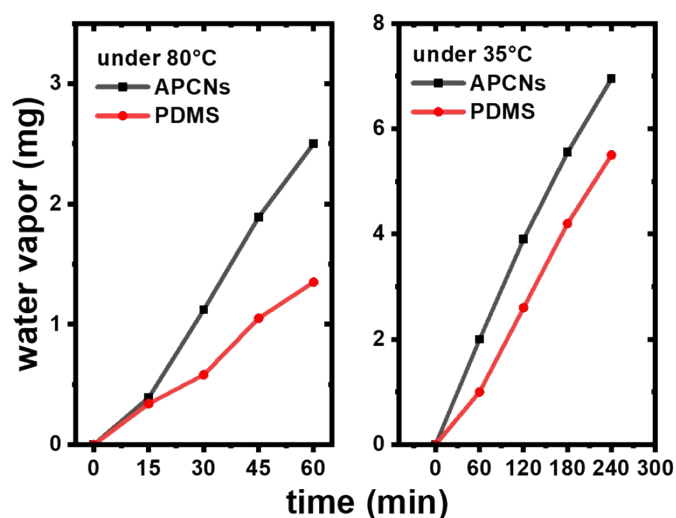


Figure S3. Water vapor permeation comparison between APCNs and PDMS.

2. Solar cells power conversion efficiency (PCE)

2.1 Raw data

All the measured PCE raw data of side, top, and bottom geometries and various set-ups in each geometry are listed as follows.

2.1.1 Side

Table S1. PCE of N719 based FDSSCs before and after side-attached LSCs with various lengths.

	APCNs LSCs	20 mm	15 mm	10 mm	5 mm
N719-1	Before	7.81	7.45	7.09	6.81
	After	10.78	9.92	8.76	7.90
N719-2	Before	7.12	6.92	6.75	6.60
	After	10.01	9.27	8.90	7.42
N719-3	Before	7.68	7.57	7.35	7.08
	After	10.69	9.84	9.03	8.09
N719-4	Before	6.27	6.06	5.82	5.68
	After	9.32	8.37	7.64	6.75
N719-5	Before	8.10	7.65	7.47	7.31
	After	11.51	10.38	9.66	8.41
N719-6	Before	6.83	6.62	6.53	6.52
	After	9.59	9.01	8.51	7.52
N719-7	Before	6.08	5.94	5.73	5.64

	After	8.6	8.28	7.56	6.39
N719-8	Before	6.05	5.84	5.62	5.56
	After	8.94	8.34	7.34	6.65

Table S2. PCE of Y123 based FDSSCs before and after side-attached LSCs with various lengths.

	APCNs LSCs	20 mm	15 mm	10 mm	5 mm
Y123-1	Before	7.26	7.45	7.62	7.59
	After	10	9.6	9.17	8.43
Y123-2	Before	6.17	6.19	6.18	6.12
	After	8.80	8.52	7.88	7.1
Y123-3	Before	6.22	6.15	6.14	6.07
	After	8.1	7.66	6.9	6.6
Y123-4	Before	5.93	6.12	6.09	5.99
	After	8.16	8.24	7.54	6.65
Y123-5	Before	8.04	8.29	8.31	8.2
	After	11.35	10.35	10.06	9.06
Y123-6	Before	6.91	7.08	7.30	7.38
	After	9.85	9.44	9.21	8.18
Y123-7	Before	6.13	6.24	6.33	6.21
	After	8.48	8.28	7.79	6.90
Y123-8	Before	7.27	7.65	7.73	7.77
	After	9.54	9.73	9.34	8.42
Y123-9	Before	6.59	6.54	6.49	6.42
	After	8.7	8.17	7.67	6.98
Y123-10	Before	7.71	7.57	7.41	6.89
	After	10.01	9.6	8.61	7.44
Y123-11	Before	6.87	6.85	6.86	6.81
	After	9.61	9.15	8.42	7.51

2.1.2 Top

Table S3. PCE of N719 based FDSSCs before and after various top-covered LSCs thickness.

	APCNs LSCs	600 um	400 um	200 um
N719-1	Before	6.57	6.44	6.27
	After	5.25	5.81	5.98
N719-2	Before	6.17	5.91	5.31
	After	5.25	5.39	5.06
N719-3	Before	6.49	6.28	4.84
	After	5.22	5.65	4.52
N719-4	Before	5.01	5.76	6.07
	After	4.01	4.91	5.72
N719-5	Before	6.41	6.78	6.61
	After	5.19	6.16	6.42
N719-6	Before	6.28	7.47	8.31
	After	5.33	6.89	7.96
N719-7	Before	7.61	8.31	9.04
	After	6.36	7.28	8.53
N719-8	Before	6.07	6.44	6.76
	After	5.03	5.74	6.49
N719-9	Before	7.94	7.71	8.00
	After	6.81	7.14	7.62
N719-10	Before	7.44	7.92	8.36
	After	6.17	7.18	8.03

Table S4. PCE of Y123 based FDSSCs before and after various top-covered LSCs thickness.

	APCNs LSCs	600 um	400 um	200 um
Y123-1	Before	7.48	7.41	7.17
	After	5.78	6.0	6.52
Y123-2	Before	6.01	5.94	5.53
	After	4.87	4.98	4.97
Y123-3	Before	5.32	5.73	6.09
	After	4.14	4.97	5.63
Y123-4	Before	7.58	7.64	7.62
	After	5.82	6.56	6.68
Y123-5	Before	6.55	6.58	6.60
	After	4.95	5.38	6.00
Y123-6	Before	7.75	7.49	7.19
	After	5.66	6.04	6.57
Y123-7	Before	6.86	6.65	6.56
	After	5.28	5.47	5.88
Y123-8	Before	7.46	7.41	7.34
	After	5.63	6.05	6.46

2.1.3 Bottom

Table S5. PCE of N719 based FDSSCs before and after various bottom-attached LSCs position.

	3rd	2nd	1st	Direct down	Without LCS
N719-1	7.24	7.02	6.75	6.41	6.28
N719-2	7.50	7.32	7.06	6.72	6.49
N719-3	7.02	6.83	6.59	6.30	6.17
N719-4	6.91	6.65	6.32	6.14	6.05
N719-5	6.63	6.59	6.46	6.10	6.01
N719-6	7.54	7.41	7.25	6.87	6.78
N719-7	7.39	7.20	6.97	6.65	6.46
N719-8	7.20	7.02	6.75	6.42	6.27

Table S6. PCE of Y123 based FDSSCs before and after various bottom-attached LSCs position.

	3rd	2nd	1st	Direct down	Without LCS
Y123-1	7.98	7.88	7.72	7.48	7.46
Y123-2	6.52	6.42	6.21	6.01	5.98
Y123-3	7.22	7.08	6.88	6.72	6.69
Y123-4	7.43	7.32	7.18	7.01	6.97
Y123-5	7.00	6.95	6.89	6.75	6.63
Y123-6	8.43	8.29	8.09	7.78	7.66
Y123-7	7.60	7.58	7.54	7.40	7.28
Y123-8	7.22	7.14	6.97	6.73	6.61
Y123-9	6.96	6.92	6.79	6.73	6.63
Y123-10	7.15	7.01	6.96	6.89	6.81
Y123-11	7.69	7.66	7.55	7.49	7.33

2.2 Statistics

Descriptive statistics is shown for all samples at Table S7. t-tests for two independent samples were performed and the results are summarized at Table S8. All tests yielded significant differences. Tests were performed for pairs of same attachment type, e.g., LSC 5 mm long, side-attachment on FDSSC N719 \times LSC 5 mm long, side-attachment on FDSSC Y123.

Table S7. Descriptive statistics of PCE enhancement for all samples.

FDSSC Type	Attachment	Length (mm)	Δ PCE (%)			n
			Mean	sd	Median	
N719	Side	5	15.6	2.6	15.2	8
		10	29.0	3.7	30.5	8
		15	36.15	3.98	35.89	8
		20	42.27	3.88	41.02	8
		Thickness (μ m)				
	Top	200	-4.71	1.07	-4.67	10
		400	-10.03	2.20	-9.56	10
		600	-17.36	2.20	-17.10	10
		Position				
	Bot	1	2.17	0.77	2.09	8
		2	7.19	1.26	7.49	8
		3	10.94	1.25	11.08	8
		4	13.70	1.92	14.31	8
Y123		Length (mm)				
	Side	5	10.42	2.21	10.49	11
		10	21.12	4.36	21.06	11
		15	29.92	4.61	28.86	11
		20	36.66	4.95	37.74	11
		Thickness (μ m)				
	Top	200	-9.89	1.65	-9.61	8
		400	-17.04	2.28	-17.99	8
		600	-23.26	2.29	-23.13	8
		Position				
	Bot	1	1.23	0.67	1.51	11
		2	3.58	1.11	3.49	11
		3	5.53	1.70	5.02	11
4		6.79	2.00	6.60	11	

Table S8. Results of t -tests for two independent samples (N719 \times Y123) for each geometry. * $p < 0.05$; ** $p < 0.01$

Side length (cm)				Top thickness (μm)			Bottom position			
0.5	1	1.5	2	200	400	600	1	2	3	4
**	**	**	*	**	**	**	*	**	**	**

2.3 EQE and dark current

The EQE of N719 and Y123 FDSSCs are reported in Figure S4. The EQE results fit well with the spectral responsiveness discussion that the LSCs maximum emission peak at 520 nm could be better used by N719 than Y123, leading to a different degree of PCE variation.

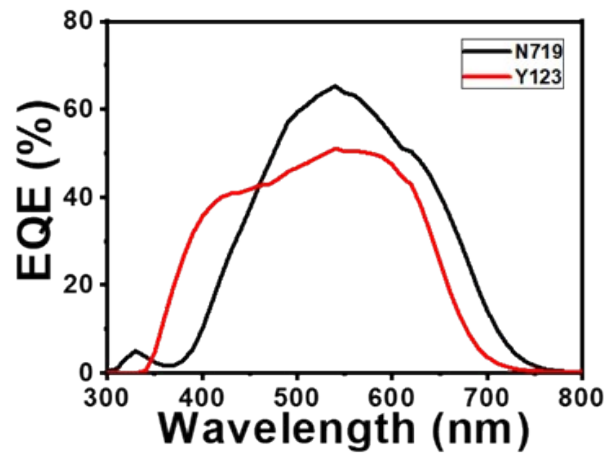


Figure S4. EQE of the N719 and Y123 FDSSCs.

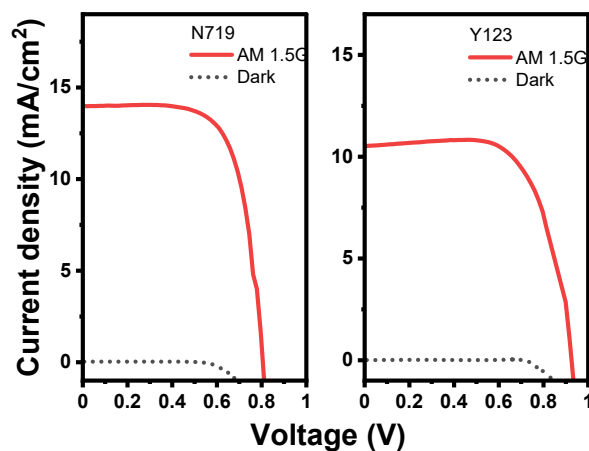


Figure S5. Dark current of the N719 and Y123 FDSSCs.

2.4 Double-sided LSCs PCE enhancement

The two-side-attached J-V curves for both N719 and Y123 are shown in Figure S5. The PCE enhancement of one-side-attached, and two-side-attached for N719 are 44.4 % and 83.9 %; and for Y123 are 37.9 % and 76.0 %. This fits well with our simulation of two-side attached LSC enhancing the PCE twice as much as one-side attachment.

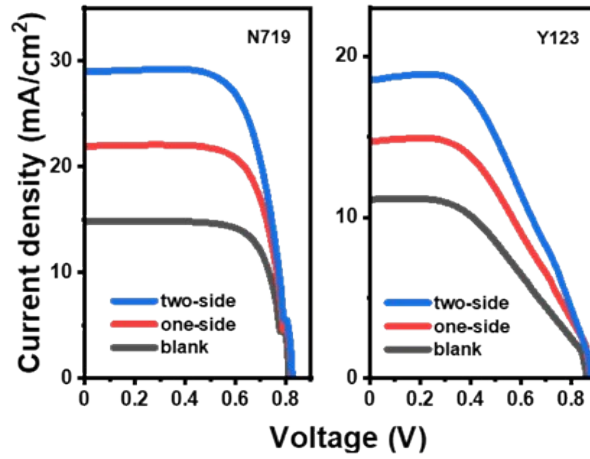


Figure S6. J-V curves of N719 and Y123 based FDSSCs, one-side attached, and two-side attached with LSCs.

2.5 Experimental and simulated photon numbers comparison

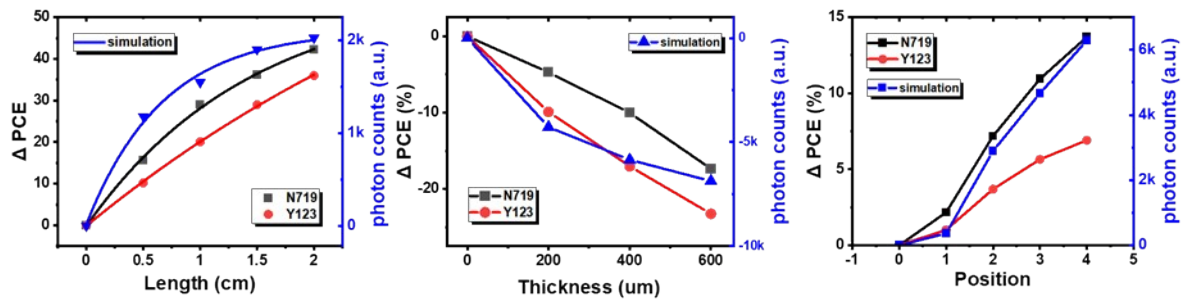


Figure S7. Experimental PCE and simulated photon number variation of FDSSCs with (a) side-attached, (b) top-covered, and (c) bottom-attached LSCs.

2.6 Parameters and defining equations

Parameter	Equation
Power conversion efficiency (PCE)	$\text{PCE} = \frac{P_{max}}{P_{in}} = \frac{I_{sc} V_{oc} FF}{P_{in} A_{FDSSC}} = \frac{J_{sc} V_{oc} FF}{P_{in}}$
Geometry factor (G)	$G = \frac{A_{front}}{A_{edge}} = \frac{A_{LSC}}{A_{FDSSC}}$
Concentration factor (C)*	$C = \frac{P_{LSC}}{P_{FDSSC}} = \frac{I_{sc,LSC} V_{oc,LSC} FF_{LSC}}{I_{sc,FDSSC} V_{oc,FDSSC} FF_{FDSSC}} \approx \frac{I_{LSC}}{I_{FDSSC}}$
Device optical efficiency (η_{opt})	$\eta_{opt} = \frac{C}{G}$

Table S9. Parameters and defining equations used in this manuscript.

* Adding light from LSCs to FDSSCs will not change the intrinsic properties of the solar cells, hence the Voc and FF are theoretically maintained before and after the LSC attachment.

3. Ray-tracing

3.1 Monte-Carlo

The Monte-Carlo ray-tracing presented in the paper was done using the open-source software pvtrace 2.0.4, a powerful Python procedure used to simulate the behavior of solar concentrators.^[2] In the simulation, the LSCs structure is built as the parameters performed in the experiments, i.e., 0-20 mm wide, 15 mm long, 1 mm thick for side tests; 1 mm wide, 15 mm long, 0-600 um thick for top tests; 1-4 mm wide, 15 mm long, 200 um thick for bottom tests. The illumination for all simulations is under AM 1.5 spectrum (National Renewable Energy Laboratory, USA) with a spot size of 25 mm² to cover whole testing area, resembling the PCE experiments using solar simulator. The LSCs polymer matrix has a defined absorption coefficient in the relevant spectral range (300–800 nm), with a quantum yield of 0. The luminescent dye absorbance spectrum was analyzed lying flat on the lid of a well-plate on Cary 50 Bio UV-visible (Agilent, USA). The measured spectrum is shown in Fig. 1 (e). The FDSSCs structure in the simulation is a rod with 0.5 mm diameter and 15 mm length, the same scale in the experiments. Besides, to monitor the photons captured by the fiber, FDSSCs are set to have infinite absorbance coefficient. For each ray-tracing simulation, 10⁵ incident photons were applied. Those photons, upon passing through the device, had a chance to be absorbed and re-emitted as a photon corresponding to the experimentally characterized spectrum. The photons, after being waveguided within the LSC or directly captured, were counted at the surface of FDSSCs.

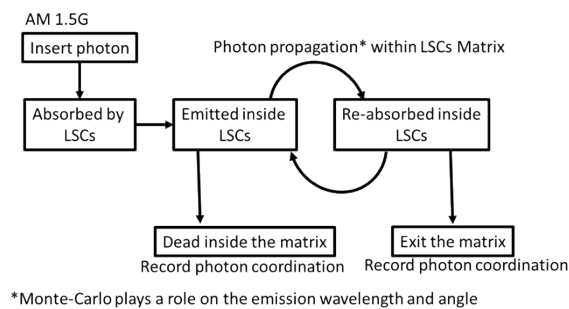
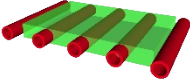
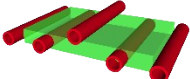
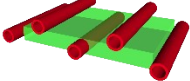
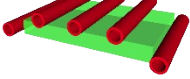
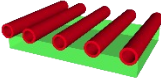


Figure S8. Monte-Carlo ray tracing flow diagram

3.2 Ray-tracing screening for optimal photon harvesting

The ray-tracing simulation for screening the optimal geometry under the LSCs size of 20 mm wide, 15 mm long, and 1 mm thick with 5 FDSSCs attached within the device. The result shows the configuration 4 is the one with highest enhanced photon harvested. As shown at Table S10 and S11, the simulation has been done, respectively, from the aspect of various fibers configuration under constant LSCs size and various fibers packing density (LSCs sizes) under constant fibers configuration. On one hand, under constant size of 3 cm² LSCs, from the photons termination recorded on FDSSCs model, the highest photon harvesting ability is the configuration of 2 fibers at the side and 3 fibers at the top of LSCs. On the other hand, with various LSCs' width to change the fibers packing density, simulation shows the optimal width is 2 cm for 1.5 cm long FDSSCs under this obtained configuration. For dense packing, less incoming photons can be absorbed by the small area LSCs and incoming photons are more probable to be blocked by top-positioned FDSSC. For loosely packed FDSSCs, on account of the self-absorption loss within the LSCs matrix, photons reach the FDSSCs do not increased proportionally to the LSCs area. Indeed, more engineering tasks and design of experiments (DOE) could be performed to figure out the optimal case for individual application, Herein, we provide preliminary investigation and insightful example for future large area integrated electronic devices.

Table S10. Five geometries of possible arrangement of FDSSCs with LSCs and the respectively enhanced photon harvesting ability.

Configuration	Δ Photon counts
1 	50 %
2 	46 %
3 	52 %
4 	62 %
5 	32 %

3.3 Ray-tracing screening for various LSCs width photon harvesting

The ray-tracing simulation for various widths, 0.5, 1, 2, 3, 5, 10 cm under the LSCs size of 15 mm long, and 1 mm thick with 5 FDSSCs attached within the device as in configuration 4 (Table S10) is investigated.

Furthermore, the optimized device of 5 FDSSCs, configuration 4, and 3 cm² LSCs, is with 0.89 mW output and 0.29% device PCE.

Table S11. Effect of the LSCs area and fibers packing density on the efficiency of the device.

LSCs width (cm)	LSCs area (cm²)	Packing density (LSCs area/ fiber number)	Δ_Photon counts (%)	Δ_Photon counts per area (cts/ LSCs area) (%/cm²)
0.5	0.75	0.15	8	11
1	1.5	0.3	23	15
2	3	0.6	62	21
3	4.5	0.9	71	16
5	7.5	1.5	77	10
10	15	3	79	5

References

- [1] (a) K. Schöller, S. Küpfer, L. Baumann, P.M. Hoyer, D. de Courten, R.M. Rossi, A. Vetushka, M. Wolf, N. Bruns, and L.J. Scherer, *Adv. Funct. Mater.*, **2014**, *24*, 5194; (b) S. Ulrich, A. Osypova, G. Panzarasa, R.M. Rossi, N. Bruns, and L.F. Boesel, *Macromol. Rapid Commun.*, **2019**, *40*, 1900360; (c) S. Ulrich, A. Sadeghpour, R.M. Rossi, N. Bruns, and L.F. Boesel, *Macromolecules*, **2018**, *51*, 5267.
- [2] D. J. Farrell, “D J Farrell, pvtrace: optical ray tracing for luminescent materials and spectral converter photovoltaic devices, <https://github.com/danieljfarrell/pvtrace>.” 2019.